

# Coherent Inverse Photoemission Spectrum for Gutzwiller Projected Superconductors

Seiji Yunoki

*Istituto Nazionale per la Fisica della Materia (INFM) and International School for Advanced Studies (SISSA), via Beirut 4, 34014 Trieste, Italy*

(Dated: November 20, 2018)

Rigorous relations for Gutzwiller projected BCS states are derived. The obtained results do not depend on the details of model systems, but solely on the wave functions. Based on the derived relations, physical consequences are discussed for strongly correlated superconducting states such as high- $T_C$  cuprate superconductors.

PACS numbers: 71.10.-w, 74.20.-z, 74.20.Mn, 74.72.-h

Right after the discovery of high- $T_C$  cuprate superconductors [1], Anderson has proposed a Gutzwiller projected BCS wave function — a quantum many-body state incorporating strong on-site Coulomb repulsion — to describe the superconducting state [2]. Since then there have been extensive studies in understanding the nature of this state and its variants [3, 4]. In addition, several reports have shown that this projected BCS wave function is indeed a good variational ansatz state to describe the ground state of  $t$ - $J$  like models [5, 6, 7, 8], which are believed to capture the low energy physics of the cuprates [9]. Although these projected BCS states were proposed more than 15 years ago, very recently they have acquired a revived interest [10, 11, 12, 13]. This is probably because recent expensive numerical calculations based on the Gutzwiller projected variational ansatz clearly indicate that many aspects of the physics of high- $T_C$  cuprate superconductors can be understood within this framework [10].

In this short communication some rigorous relations are derived for the Gutzwiller projected BCS states. It is shown that, as a consequence of the derived relations, the one-particle added excitation spectrum tends to be more coherent than the one-particle removed excitation spectrum does. It is further shown numerically that this trend is still observed approximately for more involved Gutzwiller projected BCS states. Possible experimental implications of the present results are also discussed.

Here our general system consists of a single orbital per unit cell on the two-dimensional (2D) square lattice with  $L$  sites [14]. The creation and annihilation operators of spin  $\sigma$  ( $=\uparrow, \downarrow$ ) particle at site  $\mathbf{i}$  are denoted by  $\hat{c}_{\mathbf{i}\sigma}^\dagger$  and  $\hat{c}_{\mathbf{i}\sigma}$ , respectively. A Gutzwiller projected BCS state with  $N$  particles is described by

$$|\Psi_0^{(N)}\rangle = \hat{P}_N \hat{P}_G |\text{BCS}\rangle, \quad (1)$$

where  $\hat{P}_N$  is the projection operator onto the fixed number  $N$  of particles,  $\hat{P}_G = \prod_{\mathbf{i}} (1 - \hat{n}_{\mathbf{i}\uparrow} \hat{n}_{\mathbf{i}\downarrow})$  is the Gutzwiller projection operator to restrict the Hilbert space with no double occupancy on each site, and  $\hat{n}_{\mathbf{i}\sigma} = \hat{c}_{\mathbf{i}\sigma}^\dagger \hat{c}_{\mathbf{i}\sigma}$ .  $|\text{BCS}\rangle = \prod_{\mathbf{k}, \sigma} \hat{\gamma}_{\mathbf{k}\sigma} |0\rangle$  is the ground state of the BCS mean field Hamiltonian where

$$\begin{pmatrix} \hat{\gamma}_{\mathbf{k}\uparrow} \\ \hat{\gamma}_{-\mathbf{k}\downarrow}^\dagger \end{pmatrix} = \begin{pmatrix} u_{\mathbf{k}}^* & -v_{\mathbf{k}}^* \\ v_{\mathbf{k}} & u_{\mathbf{k}} \end{pmatrix} \begin{pmatrix} \hat{c}_{\mathbf{k}\uparrow} \\ \hat{c}_{-\mathbf{k}\downarrow}^\dagger \end{pmatrix} \quad (2)$$

are the standard Bogoliubov quasi-particle operators,  $\hat{c}_{\mathbf{k}\sigma} = \sum_{\mathbf{i}} e^{-i\mathbf{k}\cdot\mathbf{i}} \hat{c}_{\mathbf{i}\sigma} / \sqrt{L}$ ,  $|0\rangle$  is the vacuum of particles, and the singlet pairing is assumed [15]. The nature of this state has been extensively studied specially in the context of high- $T_C$  cuprates [5, 6, 7, 8, 10]

A one-particle added state with spin  $\sigma$  and momentum  $\mathbf{k}$  is similarly defined by using  $\hat{\gamma}_{\mathbf{k}\sigma}^\dagger$ :

$$|\Psi_{\mathbf{k}\sigma}^{(N+1)}\rangle = \hat{P}_{N+1} \hat{P}_G \hat{\gamma}_{\mathbf{k}\sigma}^\dagger |\text{BCS}\rangle. \quad (3)$$

This state was first proposed by Zhang, *et al* [3], followed by several others [10, 12, 16]. Hereafter the normalized wave functions for the  $N$ - and  $(N+1)$ -particle states are denoted by  $|\psi_0^{(N)}\rangle$  and  $|\psi_{\mathbf{k}\sigma}^{(N+1)}\rangle$ , respectively.

First it is useful to show that the following operator relation between  $\hat{c}_{\mathbf{k}\sigma}$  and  $\hat{c}_{\mathbf{k}\sigma}^\dagger$  holds exactly:

$$\hat{P}_G \hat{c}_{\mathbf{k}\sigma} \hat{c}_{\mathbf{k}\sigma}^\dagger \hat{P}_G = \hat{c}_{\mathbf{k}\sigma} \hat{P}_G \hat{c}_{\mathbf{k}\sigma}^\dagger + \frac{1}{L} \hat{N}_{\bar{\sigma}} \hat{P}_G. \quad (4)$$

Here  $\hat{N}_{\bar{\sigma}} = \sum_{\mathbf{i}} \hat{c}_{\mathbf{i}\bar{\sigma}}^\dagger \hat{c}_{\mathbf{i}\bar{\sigma}}$  and  $\bar{\sigma}$  stands for the opposite spin of  $\sigma$ . This is easily proved by using  $\hat{P}_G \hat{c}_{\mathbf{i}\sigma}^\dagger \hat{P}_G = \hat{P}_G \hat{c}_{\mathbf{i}\sigma}^\dagger$ .

Using the above equation (4), it is readily shown that the momentum distribution function  $n_\sigma(\mathbf{k}) = \langle \psi_0^{(N)} | \hat{c}_{\mathbf{k}\sigma}^\dagger \hat{c}_{\mathbf{k}\sigma} | \psi_0^{(N)} \rangle$  calculated for the state  $|\Psi_0^{(N)}\rangle$  is related to the state  $|\Psi_{\mathbf{k}\sigma}^{(N+1)}\rangle$  through

$$n_\sigma(\mathbf{k}) = 1 - \frac{N_{\bar{\sigma}}}{L} - |u_{\mathbf{k}}|^2 \frac{\langle \Psi_{\mathbf{k}\sigma}^{(N+1)} | \Psi_{\mathbf{k}\sigma}^{(N+1)} \rangle}{\langle \Psi_0^{(N)} | \Psi_0^{(N)} \rangle}, \quad (5)$$

where  $\hat{N}_{\bar{\sigma}} \hat{P}_G = \hat{P}_G \hat{N}_{\bar{\sigma}}$  is used.

The quasi-particle weight for the one-particle added excitation is defined by

$$Z_{\mathbf{k}\sigma}^{(+)} = \left| \langle \psi_{\mathbf{k}\sigma}^{(N+1)} | \hat{c}_{\mathbf{k}\sigma}^\dagger | \psi_0^{(N)} \rangle \right|^2. \quad (6)$$

Now we shall show that there exists a simple and exact relation between  $Z_{\mathbf{k}\sigma}^{(+)}$  and  $n_\sigma(\mathbf{k})$ . To this end, it is important to notice that since

$$\langle \Psi_{\mathbf{k}\sigma}^{(N+1)} | \hat{c}_{\mathbf{k}\sigma}^\dagger | \Psi_0^{(N)} \rangle = u_{\mathbf{k}}^* \langle \Psi_{\mathbf{k}\sigma}^{(N+1)} | \Psi_{\mathbf{k}\sigma}^{(N+1)} \rangle \quad (7)$$

$Z_{\mathbf{k}\sigma}^{(+)}$  is simplified as

$$Z_{\mathbf{k}\sigma}^{(+)} = |u_{\mathbf{k}}|^2 \frac{\langle \Psi_{\mathbf{k}\sigma}^{(N+1)} | \Psi_{\mathbf{k}\sigma}^{(N+1)} \rangle}{\langle \Psi_0^{(N)} | \Psi_0^{(N)} \rangle}. \quad (8)$$

From Eqs. (5) and (8), we finally arrive at the desired relation,

$$n_{\sigma}(\mathbf{k}) + Z_{\mathbf{k}\sigma}^{(+)} = 1 - \frac{N_{\bar{\sigma}}}{L}. \quad (9)$$

It should be emphasized that to derive the above equation we have not made either any approximations or any assumptions except for the form of the wave functions for the  $N$ - and  $(N+1)$ -particle states given by Eqs. (1) and (3), respectively.

The equation (9) is also simply verified numerically on small clusters using a Monte Carlo technique. Typical results are presented in Fig. 1. As seen in Fig. 1 and for all other cases studied, Eq. (9) is satisfied within the statistical errors.

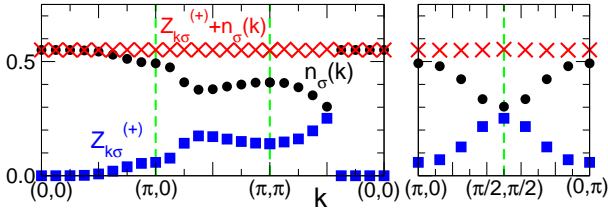


FIG. 1:  $n_{\sigma}(\mathbf{k})$  (circles) and  $Z_{\mathbf{k}\sigma}^{(+)}$  (squares) calculated using a Monte Carlo technique for  $L = 16 \times 16$  and  $N_{\uparrow} = N_{\downarrow} = 115$  [17]. The sum of the two quantities ( $n_{\sigma}(\mathbf{k}) + Z_{\mathbf{k}\sigma}^{(+)}$ ) is also plotted by crosses, which are  $1 - N_{\bar{\sigma}}/L = 0.551$  within the statistical error bars (smaller than the size of the symbols).

In order to discuss a physical consequence of Eq. (9) on the one-particle excitation spectrum, let us first derive a simple same rule. The one-particle excitation spectra for removing one particle [ $A_{\sigma}^{\text{PES}}(\mathbf{k}, \omega)$ ] and for adding one particle [ $A_{\sigma}^{\text{IPES}}(\mathbf{k}, \omega)$ ] are defined respectively by

$$A_{\sigma}^{\text{PES}}(\mathbf{k}, \omega) = -\frac{1}{\pi} \text{Im} \left\langle \hat{c}_{\mathbf{k}\sigma}^{\dagger} \frac{1}{\omega + (\hat{H} - E_0) + i0^+} \hat{c}_{\mathbf{k}\sigma} \right\rangle$$

$$A_{\sigma}^{\text{IPES}}(\mathbf{k}, \omega) = -\frac{1}{\pi} \text{Im} \left\langle \hat{c}_{\mathbf{k}\sigma} \frac{1}{\omega - (\hat{H} - E_0) + i0^+} \hat{c}_{\mathbf{k}\sigma}^{\dagger} \right\rangle,$$

where  $\langle \hat{O} \rangle$  is the expectation value of  $\hat{O}$  for the exact ground state of the system described by Hamiltonian  $\hat{H}$  with its eigenvalue  $E_0$ . It is generally proved that for any model systems defined within the restricted Hilbert space with no double occupancy on any sites by particles, such as the  $t$ - $J$  model, the 0-th moment of the spectral

function satisfies the following sum rules:

$$\int_{-\infty}^{\infty} A_{\sigma}^{\text{PES}}(\mathbf{k}, \omega) d\omega = \langle \hat{c}_{\mathbf{k}\sigma}^{\dagger} \hat{c}_{\mathbf{k}\sigma} \rangle \quad (10)$$

$$\int_{-\infty}^{\infty} A_{\sigma}^{\text{total}}(\mathbf{k}, \omega) d\omega = 1 - N_{\bar{\sigma}}/L, \quad (11)$$

where  $A_{\sigma}^{\text{total}}(\mathbf{k}, \omega) = A_{\sigma}^{\text{PES}}(\mathbf{k}, \omega) + A_{\sigma}^{\text{IPES}}(\mathbf{k}, \omega)$ . The latter equation is easily proved by using Eq. (4). Eq. (10) is a rather standard sum rule, while Eq. (11) is due to the reduction of the Hilbert space by  $\hat{P}_G$  and it is indeed satisfied for, *e.g.*, the  $t$ - $J$  model [18].

Let us now discuss what physical consequences would be expected. First we assume that there exists a system for which the ground state and the low-lying excited states are approximately described by the wave functions, Eqs. (1) and (3), introduced above. Then it follows immediately from Eqs. (9)–(11) that

$$\int_{-\infty}^{\infty} A_{\sigma}^{\text{IPES}}(\mathbf{k}, \omega) d\omega = Z_{\mathbf{k}\sigma}^{(+)}. \quad (12)$$

This relation implies that the one-particle added excitation spectrum is all coherent since only one state contributes to  $A_{\sigma}^{\text{IPES}}(\mathbf{k}, \omega)$ . It should be noted here that while several studies have recently reached the similar conclusions [12, 13], the argument presented here is more rigorous and transparent.

Next we shall discuss to what extent Eq. (9) holds and therefore Eq. (12) remains approximately true for more involved wave functions. A natural and important extension of the simplest Gutzwiller projected BCS states described by Eqs. (1) and (3) can be achieved by including charge Jastrow factors  $\hat{J}_C$ , *i.e.*,

$$|\Phi_0^{(N)}\rangle = \hat{P}_N \hat{P}_G \hat{J}_C |\text{BCS}\rangle, \quad (13)$$

$$|\Phi_{\mathbf{k}\sigma}^{(N+1)}\rangle = \hat{P}_{N+1} \hat{P}_G \hat{J}_C \hat{\gamma}_{\mathbf{k}\sigma}^{\dagger} |\text{BCS}\rangle, \quad (14)$$

for the ground state and the one-particle excited states, respectively. Here

$$\hat{J}_C = \exp \left( - \sum_{\mathbf{i}, \mathbf{j}} v_{\mathbf{i}\mathbf{j}} \hat{n}_{\mathbf{i}} \hat{n}_{\mathbf{j}} \right), \quad (15)$$

$\hat{n}_{\mathbf{i}} = \hat{n}_{\mathbf{i}\uparrow} + \hat{n}_{\mathbf{i}\downarrow}$ , and the sum runs over all the independent pairs of sites  $\mathbf{i}$  and  $\mathbf{j}$ . The importance of  $\hat{J}_C$  has been already reported for various lattice models [7, 19]. A typical example of  $v_{\mathbf{i}\mathbf{j}}$  is presented in Fig. 2 (a) where all the independent  $v_{\mathbf{i}\mathbf{j}}$  are optimized for the 2D  $t$ - $t'$ - $J$  model with  $J/t = 0.3$ ,  $t'/t = -0.2$ , and  $N_{\uparrow} = N_{\downarrow} = 115$  on  $L = 16 \times 16$  [16]. Certainly the inclusion of  $\hat{J}_C$  improves, *e.g.*, the variational energy. Besides such quantitative changes,  $\hat{J}_C$  can also make a qualitative difference. One of these examples is shown in Fig. 2 (b), where the charge structure factor  $N(\mathbf{q}) = \sum_{\mathbf{l}} \exp(-i\mathbf{q} \cdot \mathbf{l}) \langle \hat{n}_{\mathbf{l}} \hat{n}_{\mathbf{l}+\mathbf{1}} \rangle$  for small wave numbers are calculated using the wave functions with and without  $\hat{J}_C$ . As seen in Fig. 2 (b),  $N(\mathbf{q}) \rightarrow 0$

as  $|\mathbf{q}| \rightarrow 0$  for  $|\Phi_0^{(N)}\rangle$  as expected, whereas  $N(\mathbf{q}) \rightarrow \text{finite}$  as  $|\mathbf{q}| \rightarrow 0$  for  $|\Psi_0^{(N)}\rangle$  [20]. This is because  $|\text{BCS}\rangle$  does not conserve the number of particles which is instead a conserved quantity for the  $t$ - $t'$ - $J$  model [21, 22].

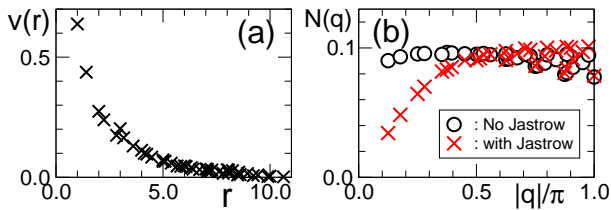


FIG. 2: (a) Charge Jastrow factor  $v(r) = v_{ij}$  as a function of distances  $r = |\mathbf{i} - \mathbf{j}|$ . These quantities are optimized in such a way that the variational energy of  $|\Phi_0^{(N)}\rangle$  is minimized for the 2D  $t$ - $t'$ - $J$  model with  $J/t = 0.3$ ,  $t'/t = -0.2$ , and  $N_\uparrow = N_\downarrow = 115$  on  $L = 16 \times 16$  [16, 17]. (b) Charge structure factor  $N(\mathbf{q})$  calculated using  $|\Psi_0^{(N)}\rangle$  (circles) and  $|\Phi_0^{(N)}\rangle$  (crosses) for the 2D  $t$ - $t'$ - $J$  model with the same model parameters as in (a). The variational parameters are optimized for both states. The statistical error bars are smaller than the size of the symbols.

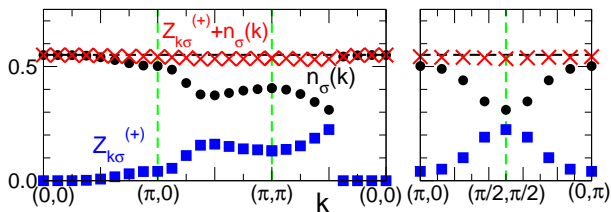


FIG. 3:  $n_\sigma(\mathbf{k})$  (circles) and  $Z_{\mathbf{k}\sigma}^{(+)}$  (squares) calculated using the wave functions  $|\Phi_0^{(N)}\rangle$  and  $|\Phi_{\mathbf{k}\sigma}^{(N+1)}\rangle$  with  $\hat{J}_C$ . The model parameters used are the same as in Fig. 2. The sum of the two quantities ( $n_\sigma(\mathbf{k}) + Z_{\mathbf{k}\sigma}^{(+)}$ ) and  $1 - N_\sigma/L = 0.551$  are also plotted by crosses and thick dashed lines, respectively. The statistical error bars are smaller than the size of the symbols.

It is now interesting to examine if the exact relation Eq. (9) proved for the states  $|\Psi_0^{(N)}\rangle$  and  $|\Psi_{\mathbf{k}\sigma}^{(N+1)}\rangle$ , and thus Eq. (12), can still hold for these more involved wave functions  $|\Phi_0^{(N)}\rangle$  and  $|\Phi_{\mathbf{k}\sigma}^{(N+1)}\rangle$ . The numerical results on small clusters are presented in Fig 3 for the 2D  $t$ - $t'$ - $J$  model with the same model parameters as in Fig. 2. As seen in Fig 3, surprisingly Eq. (9) remains satisfied, at least approximately. Thus it can be still argued that, because of the sum rule for the one-particle excitation spectrum [Eqs. (10) and (11)], Eq. (12) is approximately satisfied, and therefore most of the one-particle added excitation spectrum consists of a coherent part. Further numerical calculations have been carried out for the 2D  $t$ - $t'$ - $J$  model with different model parameters, and it was found that Eq. (9) is still satisfied within 10–15% [23].

So far we have only considered the one-particle added excitations. Let us briefly discuss the one-particle removed excitations. A one-particle removed state is analogously constructed by

$$|\Psi_{\mathbf{k}\sigma}^{(N-1)}\rangle = \hat{P}_{N-1} \hat{P}_G \hat{c}_{\mathbf{k}\sigma}^\dagger |\text{BCS}\rangle. \quad (16)$$

Although  $|\Psi_{\mathbf{k}\sigma}^{(N-1)}\rangle$  and  $|\Psi_{\mathbf{k}\sigma}^{(N+1)}\rangle$  are of very like form, the similar conclusion about the coherence of the one-particle excitations can not be drawn for the one-particle removed excitations. A simple reason for this is the following [12, 13]: for the one-particle added excitations,

$$\hat{P}_G \hat{c}_{\mathbf{k}\sigma}^\dagger |\Psi_0^{(N)}\rangle = \hat{P}_{N+1} \hat{P}_G \hat{c}_{\mathbf{k}\sigma}^\dagger |\text{BCS}\rangle \propto |\Psi_{\mathbf{k}\sigma}^{(N+1)}\rangle,$$

*i.e.*,  $\hat{P}_G \hat{c}_{\mathbf{k}\sigma}^\dagger |\Psi_0^{(N)}\rangle$  consists of only one state, while for the one-particle removed excitations  $\hat{P}_G \hat{c}_{\mathbf{k}\sigma} |\Psi_0^{(N)}\rangle = \hat{c}_{\mathbf{k}\sigma} |\Psi_0^{(N)}\rangle$ , which is not described by  $|\Psi_{-\mathbf{k}\bar{\sigma}}^{(N-1)}\rangle$  alone. It is also checked numerically on small clusters that the quasi-particle weight for the one-particle removed excitation,  $Z_{\mathbf{k}\sigma}^{(-)} = \left| \langle \psi_{-\mathbf{k}\bar{\sigma}}^{(N-1)} | \hat{c}_{\mathbf{k}\sigma} | \psi_0^{(N)} \rangle \right|^2$ , is substantially different from  $n_\sigma(\mathbf{k})$ .

Finally we shall discuss experimental implications of the present results. A most relevant experiment is angle-resolved *inverse* photoemission spectroscopy on the *superconducting state* for the *hole-doped cuprates*. If we assume that the Gutzwiller projected BCS states discussed here are faithful description for the superconducting state in the cuprates, it is expected that the inverse photoemission spectroscopy spectrum has more coherent characteristics than the direct photoemission spectroscopy spectrum does [24]. The similar trend is also expected in the *superconducting state* for the *electron-doped cuprates* except now that the *direct* photoemission spectroscopy spectrum has more coherent characteristics. This is because the  $t$ - $J$  like models can also describe the electron-doped cuprates only after the particle-hole transformation:  $\hat{c}_{\mathbf{k}\sigma} \rightarrow \hat{h}_{\mathbf{k}+\mathbf{Q}\sigma}^\dagger$  [ $\mathbf{Q} = (\pi, \pi)$ ] [25], and the same argument presented here is still true for  $\hat{h}_{\mathbf{k}\sigma}^\dagger$ .

To summarize, we have derived some rigorous relations for the Gutzwiller projected BCS states. Using a sum rule for the one-particle excitation spectrum, it was shown that the one-particle added excitation spectrum tends to be more coherent than the one-particle removed excitation does. Possible experimental implications were also discussed. Finally, it should be noted that all the results presented here are based on the Gutzwiller projected BCS states studied, and a question of whether these states can represent the exact eigenstates of some particular model Hamiltonian is beyond the scope of the present study.

The author is grateful to S. Sorella, R. Hlubina, and E. Dagotto for stimulating discussions. This work was supported in part by INFM through contract n. OA04007678.

- 
- [1] J. G. Bednorz and K. A. Müller, Z. Phys. B **64**, 189 (1986).
- [2] P. W. Anderson, Science **235**, 1196 (1987).
- [3] F. C. Zhang, C. Gros, T. M. Rice, and H. Shiba, Supercond Sci. Technol. **1**, 36 (1988).
- [4] For a recent review, see, *e.g.*, P. A. Lee, N. Nagaosa, and X.-G. Wen, cond-mat/0410445, and references therein.
- [5] C. Gros Ann. of phys. (N.Y.), **189**, 53 (1989).
- [6] H. Yokoyama and M. Ogata, J. Phys. Soc. Jpn. **65**, 3615 (1996).
- [7] S. Sorella, G. B. Martins, F. Becca, C. Gazza, L. Capriotti, A. Parola, and E. Dagotto, Phys. Rev. Lett. **88**, 117002 (2002).
- [8] C. T. Shih, T. K. Lee, R. Eder, C.-Y. Mou, and Y. C. Chen, Phys. Rev. Lett. **92** 227002 (2004).
- [9] F. C. Zhang and T. M. Rice, Phys. Rev. B **37**, R3759 (1988).
- [10] A. Paramekanti, M. Randeria, and N. Trivedi, Phys. Rev. Lett. **87**, 217002 (2001); Phys. Rev. B **70**, 054504 (2004).
- [11] P. W. Anderson, P. A. Lee, M. Randeria, T. M. Rice, N. Trivedi, and F. C. Zhang, J. Phys. Condens. Matter **16**, R755 (2004).
- [12] P. W. Anderson and N. P. Ong, cond-mat/0405518.
- [13] M. Randeria, R. Sensarma, N. Trivedi, and F.-C. Zhang, cond-mat/0412096.
- [14] Even though the 2D square lattice is considered in this paper, the results presented here for the projected BCS states without charge Jastrow factor  $\hat{J}_C$  can be also applied on any spatial dimensions with any lattice geometry.
- [15] See, *e.g.*, *Theory of Superconductivity*, by J. R. Schrieffer, (Addison-Wesley, New York, 1988).
- [16] S. Yunoki, E. Dagotto, and S. Sorella, Phys. Rev. Lett. **94**, 037001 (2005).
- [17] Following the standard BCS theory with  $d$ -wave pairing [15],  $|u_{\mathbf{k}}|^2 = [1 + \xi_{\mathbf{k}}/E_{\mathbf{k}}]/2$  and  $|v_{\mathbf{k}}|^2 = [1 - \xi_{\mathbf{k}}/E_{\mathbf{k}}]/2$  are parameterized by  $E_{\mathbf{k}} = \sqrt{\xi_{\mathbf{k}}^2 + |\Delta_{\mathbf{k}}|^2}$ ,  $\xi_{\mathbf{k}} = -2t(\cos k_x + \cos k_y) - 4t' \cos 2k_x \cos 2k_y - \mu$ , and  $\Delta_{\mathbf{k}} = \Delta(\cos k_x - \cos k_y)$ . For the calculations presented in Fig. 1,  $\Delta/t = 0.448$ ,  $t'/t = -0.302$ , and  $\mu/t = -0.675$  are chosen, which are optimized variational parameters for the 2D  $t$ - $t'$ - $J$  model with  $J/t = 0.3$  and  $t'/t = -0.2$  [16].
- [18] W. Stephan and P. Horsch, Phys. Rev. Lett. **66**, 2258 (1991).
- [19] M. Capello, F. Becca, M. Fabrizio, S. Sorella, and E. Tosatti, Phys. Rev. Lett. **94**, 026406 (2005).
- [20] This asymptotic behavior of  $N(\mathbf{q})$  has been observed for various lattice sizes used.
- [21] S. Sorella, private communication. See also, for example, Ref. [15] in Chapter 8.
- [22] Within cluster sizes used ( $L$  up to 450), it is found that  $v(r)$  can be fitted by  $a_0 + a_1/r$ , where  $a_0$  and  $a_1$  are fitting parameters. Based on a RPA treatment [19], the long-range nature of  $v(r) \sim 1/r$  in  $|\Phi_0^{(N)}\rangle$  can alter the small  $|\mathbf{q}|$  behavior of  $N(\mathbf{q})$  for |BCS) to  $N(\mathbf{q}) \sim |\mathbf{q}|$ , which is in good agreement with the present numerical calculations presented in Fig. 2 (b).
- [23] An important counter example is found in one-dimensional interacting lattice systems where the Gutzwiller projected states with singular Jastrow factor  $v(r) \sim \ln|r|$  can describe the Tomonaga-Luttinger physics [see, for example, C. S. Hellberg and E. J. Mele, Phys. Rev. Lett. **67**, 2080 (1991)].
- [24] Due to the coupling to other degrees of freedom such as phonons, presumably the spectrum gets broadened.
- [25] T. Tohyama, S. Maekawa, Phys. Rev. B **49**, 3596 (1994); R. J. Gooding, K. J. E. Vos, P. W. Leung, Phys. Rev. B **50**, 12866 (1994).